An Investigation on the Effect of Steric Bulk on the Mechanism for Nucleophilic Substitution of Histidine Derivatives on N-HydroxySuccinimide Esters Tethered to Silver Nanoparticle Surfaces

By
Benjamin Thomas Blackburn
Department of Chemistry
Allegheny College
Meadville, Pennsylvania

April, 23, 2021

Submitted in fulfillment of the senior thesis requirements of the Department of Chemistry at Allegheny College and approved by the senior thesis committee.

_____	_____	_____	_____
Dr. Comp Advisor	**Date**	***Dr. 2nd Reader***	**Date**

_____Benjamin T. Blackburn_____
Pledge

Table of Contents

Background and Significance

Introduction to Biosensors …… 2

Kinetic Modeling for Mechanism Determinace…….…….... 4

Nanoparticle Formation and Capping Agents……..…….. 9

Raman Spectroscopy and SERS……....…….…..... 10

Specific Aims

Aim 1……....14

Aim 2……..……..14

Aim 3……...……....15

Experimental Design

Overview……....…….……..17

Synthesis of Nanoparticle Surfaces…….…….…….……17

Trials With Peptides…….…….19

Preliminary Results

Trials with Histidine…….…..22

Trials with Histidine-Glycine…….24

Overall Conclusions……..…….26

Proposals for Future Research…….……..……27

Acknowledgements …….……....30

References …….....31

Background and Significance

Introduction to Biosensors

Reactions involving biosensors are a relevant area of research in modern chemistry.[1-8] Biosensors are used for finding the amount of an analyte within a particular body of matter. Depending upon their composition, a biosensor can be made to detect a wide array of analytes.[1] For example, biosensors exist for monitoring glucose in blood for diabetics, measuring harmful chemicals in water, and detecting cancer cells or antibodies.[1, 2, 4] Generally speaking, all biosensors work a similar way. There is a binding analyate, recognition system, transducer, and a measurable signal.[1, 5] A model biosensor consisting of the four parts listed previously can be seen in Figure 1.

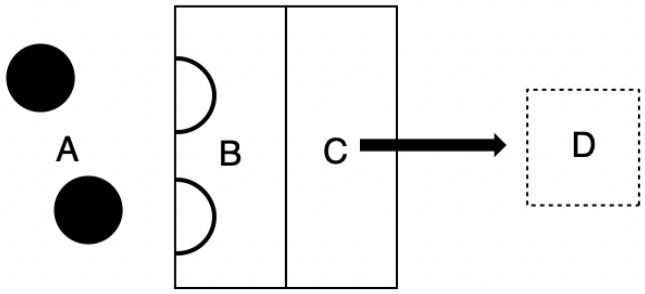


Figure 1: A general depiction of a biosensor where the analyte (A), recognition system (B), transducer (C), and measurable signal (D) are working together. [1]

When creating a biosensor, it is important for the recognition system to exclusively bind to the analyte that is being measured. For this reason, proteins that bind to a specific analyte are commonly used as recognition systems. A way of getting a protein to attach to a transducer is by utilizing a nucleophilic amino acid, like histidine.[8-14] Histidine can either be present in a protein naturally or attached to a protein through a histidine tag. These tags are typically six to eight member chains of consecutive histidine

residues artificially inserted onto proteins for their ability to coordinate with metals.[6, 9-11,15] Regardless of how present in the protein, histidine residues attach to transducer surfaces directly or through an electrophilic linking layer adsorbed to a surface.[8-15] This keeps the protein immobilized on the surface for later reactions with analyte.[9-12,16] Histidine containing proteins are relevant in medical/biological biosensor reactions due to imidazole ring side chain being deprotonated at physiological pH values.[10-11] The physiological pH activity makes biosensors with histidine containing protein recognition systems specifically pertinent for measuring analyte in human or animal cell samples.[11]

An effective recognition system and transducer connection is crucial. Once an analyte binds to a recognition system, the chemical change that occurs is converted into a measurable signal by the transducer.[1, 5] Common transducer methods are electrochemical, optical, or piezoelectric.[5] Another method of transduction is the use of metal nanoparticle surfaces that has the ability to produce a measurable signal.[3-4, 6-7, 13-14] Once the metal nanoparticle transducer gives off a signal, it can be recorded and data can be processed accordingly to tell how much analyte is present. Something important about the metal nanoparticle method is that analyte attachment is dependent upon the orientation of the adsorbed recognition system.[15] If a protein being used as a recognition system binds to the surface in a way that cannot be accessed by the analyte, the biosensor will not function. A way to control the orientation of a recognition system is to use a linking layer. This linking layer will orient the recognition system through a previously known reaction. In turn, the recognition system is presented in a way that it is known to accept an analyte instead unpredictably binding to a metal nanoparticle surface directly.[15]

Within this study, different sized histidine containing peptides will be attached to 4-Mercaptobenzoic Acid (4-MBA) capped silver nanoparticle (AgNP) surfaces using a N-Hydroxysuccinimide (NHS)/1-Ethyl-3- (3-dimethylaminopropyl)-Carbodiimide (EDC) tethering. While an NHS/EDC linking layer is commonly used to bind proteins to surfaces, little is known about its mechanism.[7-8,12] The rate laws of the attachment reactions will be investigated to determine the mechanism that various histidine containing peptides bind to surfaces. The smaller histidine containing

peptides do not accept specific analytes exclusively, and would not serve as valid recognition systems. However, knowing more about how sterrics around a histidine residue impact attachment mechanism will help predict how larger histidine tagged, or natively histidine containing proteins bind to AgNP surfaces via NHS/EDC tethering.

Kinetic Modeling for Mechanism Determinace

In order to give insight into the mechanism of attachment, a kinetic model can be used. In science, when real world phenomena are simulated using concepts of basic sciences it is called a model.[17] When kinetics are studied, the reactants that have an impact on a rate of reaction are verified. The number of reactant molecules that participate in a reaction, and have a significant impact on its rate, is called the molecularity.[18] Specifically, there will be a focus on the contrasting rate laws of unimolecular reactions (involving one molecule), and bimolecular reactions (involving two). A unimolecular reaction has a first order rate law, while a bimolecular reaction has second order. In both of these cases, the rate at which a given unimolecular and bimolecular reaction commences will be dependent upon the concentrations of the reactants that participate in it. Model rate laws for given unimolecular and bimolecular reactions can be seen in Eq 1.[18]

$$\text{Unimolecular Rate} = k[A] \quad \textbf{(1A)}$$

$$\text{Bimolecular Rate} = k[A][B] \quad \textbf{(1B)}$$

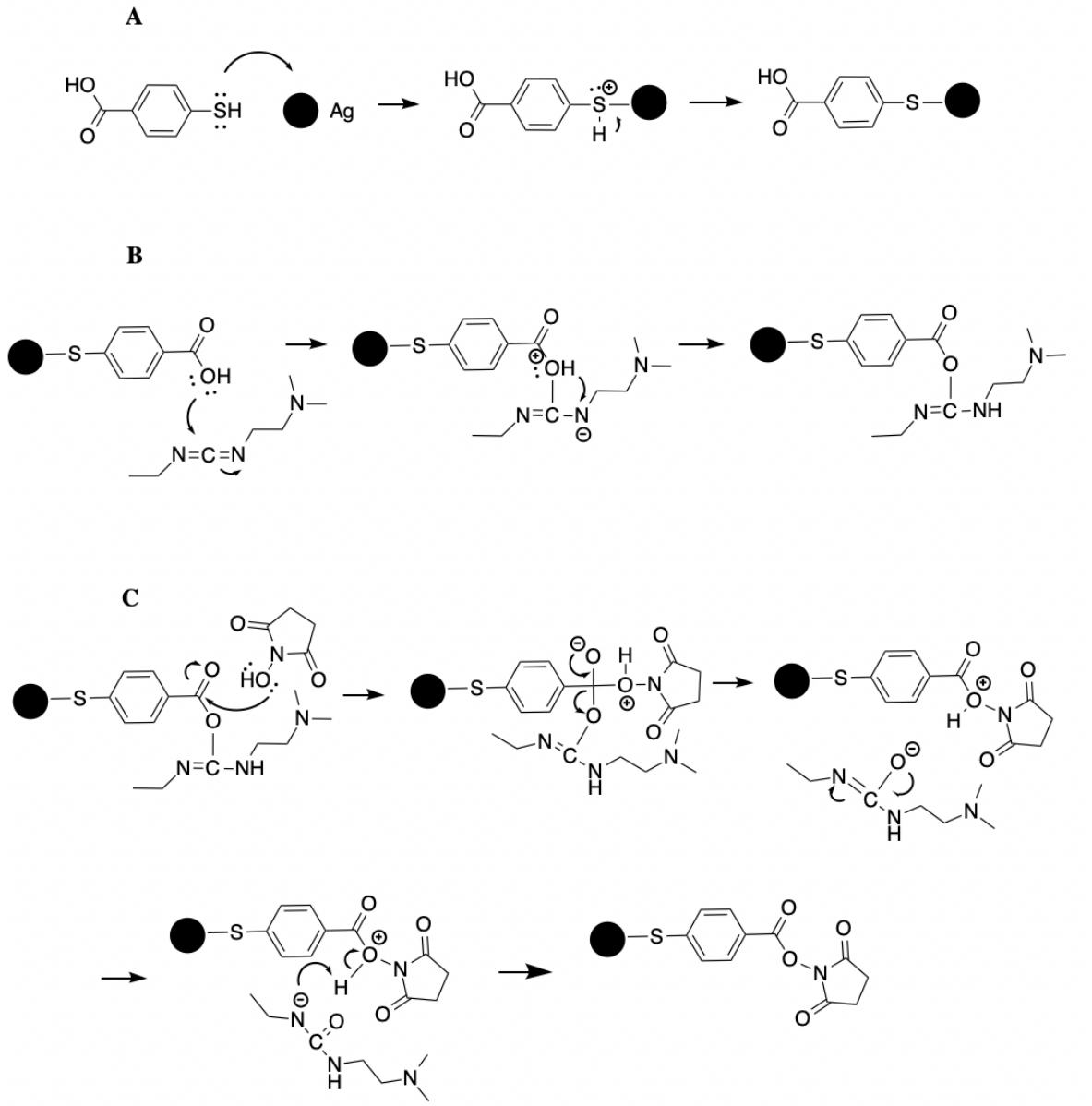
Where k is a given rate constant, it can be seen in Eq 1A that the rate is proportional to a given concentration of a single reactant, A. Conversely in Eq 1B**,** the reaction rate is dependent upon both the concentration of one reactant A, and another B. This is pertinent information in kinetic modeling because

concentration dependence can be traced throughout the course of a reaction to obtain the rate law it follows. Once rate law is given, the mechanism can be proposed.

Oftentimes in kinetic studies, what is known as a pseudo first order reaction is utilized. A pseudo first order reaction is a bimolecular reaction that has been manipulated so it is only dependent upon the concentration of one reactant.[19-20] Here, the concentration of one reactant is of such greater magnitude than the other, that it does not significantly change. Pseudo first order reactions are commonly utilized by scientists due to how easily kinetic data can be obtained by them compared to higher order reactions.[20] An observed rate of reaction (k_{obs}) can be determined at variable concentrations during a pseudo first order reaction. If the observed rate constants do not change with respect to a reactant concentration, it can be determined that the reactant is not involved within a given mechanism. However, if the observed rate constants are seen to change with respect to a given reactant concentration, it can be determined that the molecule is involved in the reaction mechanism. In this study, a pseudo first order reaction where histidine containing peptides are in greater excess to NHS esters tethered to AgNP surfaces will be utilized. The values of k_{obs} will be analyzed with respect to a changing histidine containing peptide concentration. From this, rate laws can be determined which correlates to proposed mechanisms that histidine containing peptides follow when binding to a AgNP surface via NHS/EDC tethering.

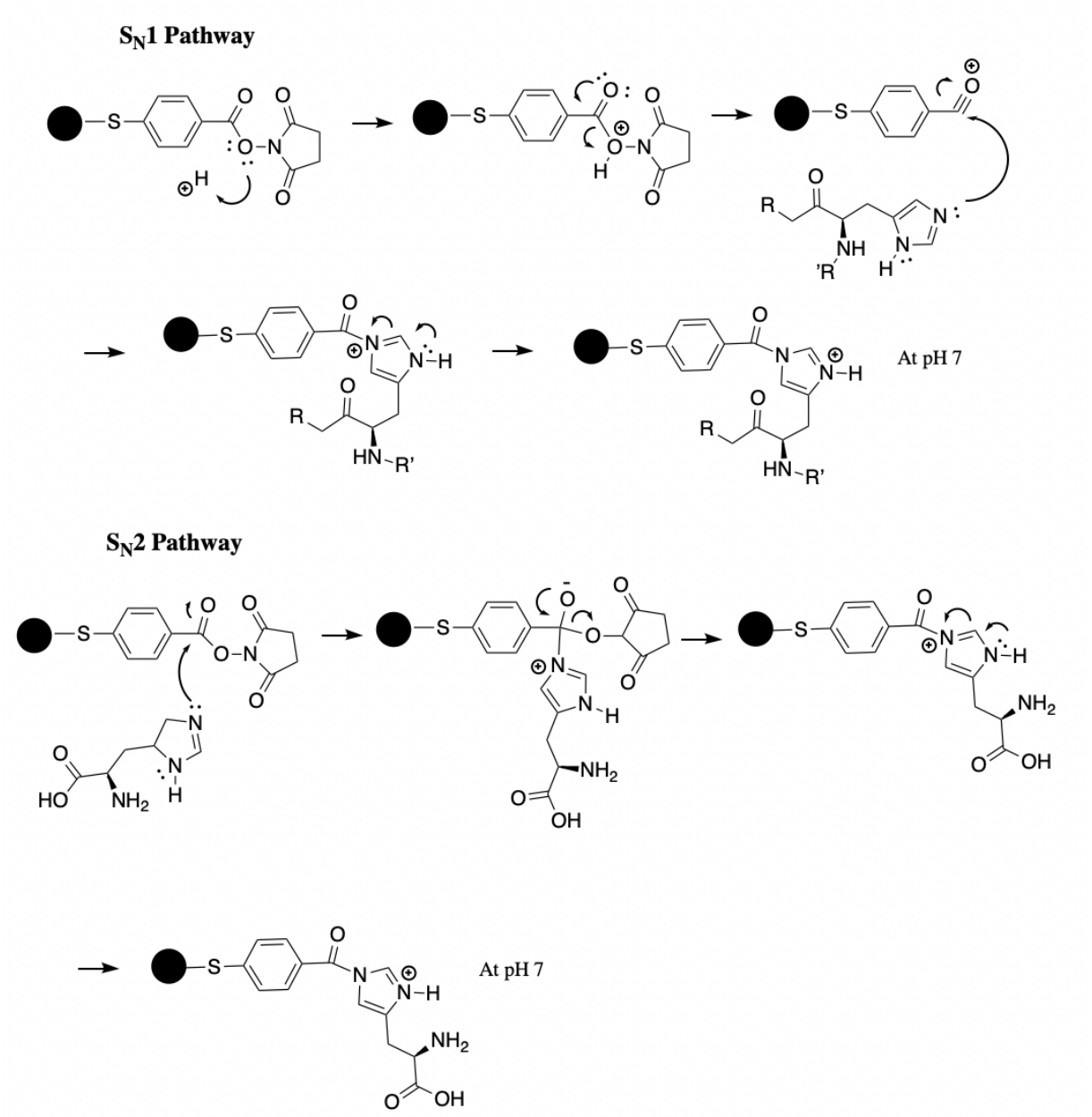
In Scheme 1 the mechanism that the NHS ester group is obtained on the surfaces is shown. The individual silver atoms on AgNP surfaces are first capped with 4-MBA, then subject to an NHS/EDC soak. The resulting product is the NHS ester connected to a silver atom in a AgNP by a thiol/benzene linker. This ester can be subject to substitution reactions that will link nucleophilic peptides to the capped AgNP surface.

Scheme 1: NHS Ester Preparation on AgNPs



It has been shown that a single histidine amino acid binds to a NHS/EDC prepared AgNP in solution according to bimolecular substitution (S_N2) reaction.[12] However, with larger histidine containing proteins, like glucose oxidase, the tethering reaction shows evidence for a unimolecular substitution mechanism (S_N1).[12] Scheme 2 shows a depiction of the S_N1 and S_N2 pathways that a histidine containing protein could follow when being tethered to a AgNP surface via NHS/EDC.

Scheme 2: Substitution Reactions of Histidine Based Peptides



The S_N1 pathway for larger peptides shows a proton from solution (H_2O) reacting with the ester, forming the acylium ion ($C{\equiv}O^+$), followed by substitution by the histidine containing peptide.[12] Other portions of

the larger protein are represented by R and R'. The S_N2 pathway for smaller peptides shows initial attachment of histidine, followed by the collapse of a tetrahedral intermediate that ultimately ejects NHS. The acylium ion that forms within the S_N1 pathway is of importance. It is a highly unstable and reactive species. If present in the mechanism, it will likely give rise to side reactions where molecules other than the histidine containing peptide are tethered to the AgNP surface. If the acylium ion is proposed to be present in a peptide attachment mechanism, precautions can be taken to limit side reactions. There would then be better control of the biosensor being made. For this reason, it is particularly important to find how large, or sterically hindered residues around histidine can be before the S_N1 attachment mechanism is invoked.

Within the study, three different peptides; histidine (Figure 2A), histidine-glycine (his-hly) (Figure 2B) and glycine-histidine-glycine (gly-his-gly) (Figure 2C), are proposed to determine how sterrics around a histidine residue impact the rate law of NHS/EDC prepared AgNP surface attachment.

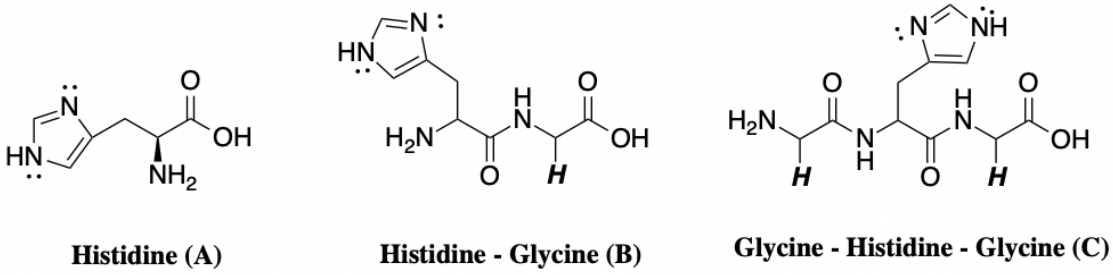


Figure 2: The increasing steric bulk around the nucleophilic histidine imidazole side chain is showcased by the addition of 1 or 2 Gly ligands. The more subtle glycine side chain/s are denoted by ***H***.

Glycine was selected as the amino acid connected to histidine because it will not conflict with the reaction between the histidine and the activated ester. The amino acid glycine does not contain any nucleophiles that could compete with the imine nitrogen (C=N) nitrogen in the histidine ring. Glycine only has a non-nucleophilic hydrogen as its side chain which would not bring about additional side reactions. The

added steric hindrance from one or two glycine residues simulate bulky regions present in larger histidine containing protein recognition systems. These bulky regions surrounding a histidine residue in larger proteins could interfere with the nucleophilic attack of the NHS ester needed for the S_N2 mechanism. When histidine is hindered so much that it does not directly attack the NHS ester, proton transfer from solvent is the predominant reaction. This leads to significant acylium ion formation and the preferential S_N1 pathway of attachment for larger proteins.[12] By seeing if the addition of one or two simple glycine residues changes rate law, or impacts rate constant, quantitative comparisons can be made with respect to a singular histidine.

Nanoparticle Formation and Capping Agents

The AgNP surface composition will play an important role in being able to obtain valid kinetic data. Nanoparticles are molecular structures measured on the 10^{-9} m (nanometer) scale.[21] Atomic silver is measured to be on the pico, or 10^{-12} m (picometer) scale. This vast difference in size means that a singular AgNP has to be made up of numerous pico scale silver atoms. Generally speaking, the nanoparticle synthesis process includes the reduction of a silver salt, aggregation, and introduction of a capping agent.[21-22] Silver will come from $AgNO_3$, and the reducing agent is hydrazine monohydrate. The reduction can be seen in Scheme 3 below.

Scheme 3: Nanoparticle Preparation via Hydrazine [22]

$$4Ag^+ + N_2H_4 \rightarrow 4Ag^0 + N_2 + 4H^+$$

The hydrazine effectively reduces the positively charged silver to its neutral state. Once neutral, the silver atoms have the ability to aggregate into nanostructures. After which, the capping agent can be introduced. A capping agent is oftentimes an organic molecule that gets adsorbed onto a metal nanostructure. They

have the ability to control aggregation of nanoparticles and limit/promote attachment of other molecules in solution.[23] As seen in Scheme 1A, 4-MBA is what will be used to cap the silver nanoparticles. 4-MBA has a few key characteristics that allow it to stabilize silver nanoparticles. Firstly, the thiol group on 4-MBA acts as a softer base compared to the oxygens in the carboxyl group.[23] This is because negatively charged sulfur has a lower charge to radius ratio compared to the negatively charged oxygen.[24] The silver at the zero charge after reduction, acts as a soft acid.[23] Neutral silver's soft acid properties are that it is a transition metal with a mostly filled 4d subshell, and a relatively large atomic radius compared to other metals.[24] The preferential soft acid/soft base interaction is what drives the thiol to attach to silver atoms within the AgNP surface instead of the carboxyl group. This explains why molecules with thiol functional groups are commonly used as capping agents or tethers on silver surfaces.[3, 8, 13, 23, 25-26] The carboxyl group is then presented outward for connection of the NHS/EDC tethering layer. Another component of the 4-MBA capping agent that plays an important role in nanoparticle stabilization is the phenyl ring. When the 4-MBA molecules are adsorbed, they are standing in an orientation that allows intermolecular interactions of phenyl rings. A phenyl ring of one 4-MBA will participate in π-π stacking noncovalent interactions with the phenyl ring of another.[23] These interactions create a more stable layer of capping agent around the AgNPs that favorably promotes the carboxylic 4-MBA substituent for NHS/EDC tethering.

Raman Spectroscopy and SERS

The progress of histidine containing peptide reactions taking place on the AgNP surfaces will be monitored using Raman Spectroscopy. Raman is a non destructive spectroscopy method that has recently become popular in monitoring reactions of biosensors.[2-4, 13-15] Raman spectroscopy relies on scattering to obtain molecular information.[27-28] Energy is measured of photons emitted from a laser spectrometer before and after it interacts (scatters) with a given sample. If photons of light are scattered with the same energy

as when they are emitted this is known as Rayleigh Scattering.[27-28] Rayleigh Scattering does not convey much information about molecular structure. This information is obtained when photons interact with sample molecules and scatter with either higher energy (Stokes) or lower energy (Anti-Stokes) compared to emission.[27-28] The difference in energy of the Stokes and Anti-Stokes scattered photons can then be used to give information about the molecular structure of the sample in solution, or on a surface.

Specifically speaking, Surface Enhanced Raman Spectroscopy (SERS) will be used for analysis. Some metal nanoparticles, including silver, have a special property called Localized Surface Plasmon Resonance (LSPR).[21-22, 29, 32] This is when the conduction electrons of individual silver atoms interact with each other within a given AgNP structure. The electrons of the individual atoms interact with others located radially around them when they are excited by visible light.[29] In SERS, the combination of the constructive plasmon interactions have the ability to enhance Raman Spectra to the power of 10^{10-11} for all peaks.[28] SERS is often used to determine interface composition. In this study, AgNP clusters will be adsorbed onto Boron Nitride Nano Sheets (BNNS).[30] As seen in Figure 3 the BNNS sheets bring the AgNP clusters closer together, thus maximizing Raman enhancement through LSPR.[30]

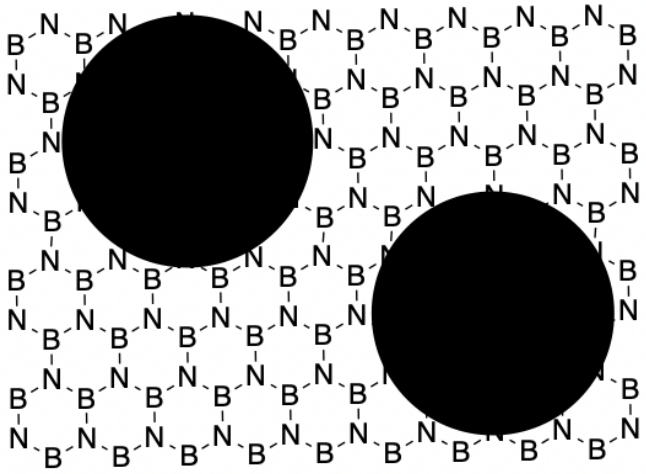


Figure 3: A general depiction of how larger AgNPs (black circles) coordinate with BNNS on surfaces before reactions take place. The AgNPs are brought closer together, furthering the effect of LSPR.

The lone pairs on the BNNS nitrogens coordinate to AgNP structures which situate them on the nanosheets through the course of reactions. The constructive plasmon interaction between AgNPs on the surface leads to strongly enhanced Raman scattering.[28,32] This effect between proximal AgNPs also explains the very low detection limits around the 10^{-12} M scale of SERS.[22] The low detection is important because as stated previously, the NHS ester adsorbed to the surface will be present at very low concentrations in order to force pseudo first order kinetics.

The very low amount of NHS ester present on the AgNP surfaces justifies the use of SERS. Knowing the composition of the AgNP surface can be utilized to make a rough estimate of the NHS ester present for peptide substitution reactions. Silver has a Face Centered Cubic (FCC) crystal structure at room temperatures.[32] Assuming that the AgNP surfaces have a densely packed FCC(100) Miller Indices, Figure (4) shows a depiction of what the surfaces would look like on an atomic level.

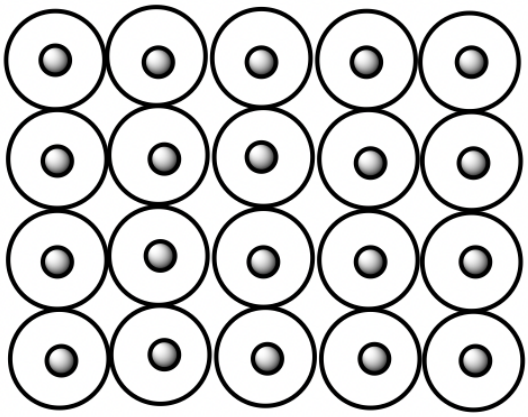


Figure 4: An aerial view of the surfaces is presented. The open circles represent silver atoms present within the FCC (100) face of one AgNP structure. The smaller, shaded circles represent 4-MBA molecules in a standing position located in "on top" sites of silver atoms.

There are 4-MBA molecules adsorbed to each of the individual silver atoms within the FCC(100) crystal structure. A silver atom has a radius of 172 pm, and a 2 dimensional area of 9.3×10^4 pm^2. Using this area, if the AgNP are packed together as closely as possible on BNNS sheets, and 4-MBA occupy sites

directly on top of each individual silver atom, the amount of 4-MBA molecules adsorbed to the surface will be on the 10^{14} scale per cm^2. Assuming that NHS/EDC tethering happens on all adsorbed 4-MBA molecules, the same amount of NHS esters (10^{14} molecules) would be presented to react with peptides. In practice, the number is likely to be lower because there will be some distance between individual AgNP structures on BNNS sheets, or side reactions that make some 4-MBA molecules not take up the NHS/EDC tether. However, even if AgNP are as close as possible, and all 4-MBA have an NHS ester, the amount of NHS esters present for reactions on surfaces would be on the 10^{-9} mol scale. This range is within the low detection limit of SERS and significantly smaller than the amount of peptide being introduced (10^{-5} mol scale). The vast concentration difference justifies the pseudo first order reaction being used. The low NHS ester concentration range could not have been detected by Raman spectroscopy without the extra surface enhancement.[22] As the reactions of histidine containing peptides progress, the Raman peak for NHS carbonyls (1770 cm^{-1}) will decrease as it acts as a leaving group, while the 4-MBA benzene peak (1590 cm^{-1}) remains constant. The high enhancement of SERS is what allows for real time kinetic data to be obtained from the Raman peaks with confidence as the reactions progress.[12] The ratio of the NHS peak height to 4-MBA is the basis for all kinetic data used to calculate rate laws and constants.

As it can be seen, there is more information to be obtained about the mechanism of attachment of histidine containing peptides to AgNP surfaces with an attached NHS ester. The mechanism can be effectively studied using strategies of kinetic modeling. The AgNP surface structure and method of SERS will play a significant role in the results sought to be obtained from this study. With rate law and proposed mechanisms of attachment, insight about the effectiveness or limitations of attaching proteins to potential biosensor transducer surfaces using NHS/EDC linkers is sought to be obtained.

Specific Aims

Aim 1: Verify that histidine attaches to NHS/EDC prepared silver nanoparticle surfaces according to S_N2 Kinetics.

In trials with 5-20 mM histidine at pH 7, observed rate constants will be obtained. This will be done through a pseudo first order reaction. The concentration of histidine will be of greater excess compared to the tethered NHS ester on AgNP surfaces. The observed rate constants from these reactions will be plotted against the varying histidine concentration. If the graph is linear, it shows that the reaction is dependent on both histidine and the NHS ester concentrations. The graph correlates to a second order reaction, and aligns with the proposed S_N2 mechanism. If the reaction between a single histidine amino acid in solution and a tethered NHS ester occurs according to S_N2 kinetics this will lay the framework for the rest of the study. Without the step of confirming the rate law, and obtaining an actual rate constant there would be no way to compare reactions of other peptides. Therefore, this initial aim will be the baseline comparison for understanding the attachment of larger histidine containing protein recognition systems to a AgNP transducer surface through NHS/EDC tethering in potential future biosensors.

Aim 2: Compare the rate constant of histidine attaching to NHS/EDC Prepared AgNP surfaces to that of AgNP in solution.

If the rate constant of histidine attachment is found for the NHS/EDC prepared AgNP surfaces it can be compared to that of 0.076 $mM^{-1}s^{-1}$ forwhen histidine binds to NHS/EDC prepared AgNP in solution.[12] The rate constant will allow for a quantitative comparison to be made between the surface and solution mediums. The comparison will show how quickly and efficiently histidine are able to bind to AgNP surfaces. With the nanoparticles in solution, both the NHS/EDC prepared AgNP and histidine are

dispersed evenly. Here, the histidine and the NHS ester are more likely to collide in the preferential orientation that results in the substitution reactions being studied. Conversely, while histidine is still dispersed evenly through solution during surface reactions, the NHS esters are immobilized. This makes the orientation between histidine and the NHS ester needed for the substitution reactions less likely to occur. If the surface reactions have lower rate constants as predicted, it can be seen how much slower or inefficient the reactions are compared to NHS/EDC prepared AgNP in solution. This comparison is important because there are advantages to having a biosensor on a pre-prepared surface compared to in solution. Not only are surface based transducers able to be used for higher enhancement spectroscopy methods like SERS, they have practical applications.[3-4, 29-30, 33-34] If all components of a biosensor are adsorbed onto a metal nanoparticle surface, it could not take lab work to use. Average people can use biosensors on a surface at home quickly for medical needs. At home biosensor technologies like glucose monitors exist using similar methods. The hassle of sending samples off to a lab or going to an office where solutions need to be measured is effectively bypassed. The rate constant of histidine attaching to NHS esters on AgNP surfaces would begin to show if this method of connecting a recognition system to a transducer is a valid path to follow for new at home biosensor technologies.

Aim 3: Analyze how the rate law or constant change as steric hindrance increases around a nucleophilic histidine residue in larger peptides.

His-gly and gly-his-gly proteins are planned to be tested alongside singular histidine residues in order to compare their rate laws. The rate law associated with the attachment reaction will allow for a mechanism to be proposed. Variance in rate law between trials of different peptides will come solely from increased steric hindrance of added glycine residues. As stated previously, there are no other competing nucleophiles with the addition of glycine that could interfere with the imine nitrogen within histidine. Steric hindrance is predicted to make the nucleophilic histidine less accessible, and block the substitution

reaction from happening once a protein is large enough. The presiding reaction instead would be the NHS ester accepting a hydrogen from solution, invoking the S_N1 peptide attachment. With the comparison between peptides, it will be seen if his-gly and gly-his-gly are large enough to attach to the surface through the S_N1 reaction (first order rate law) instead of S_N2 (second order rate law). If his-gly and gly-his-gly show evidence for first order reactions, it shows adding one or two glycine residues to histidine respectively provides enough steric hindrance to invoke a mechanistic change. Peptides larger than a singular histidine amino acid will not provide for an efficient biosensor recognition system. As shown in Scheme 2, an acylium ion is formed during S_N1 attachment. The formation of the acylium ion can lead to side reactions, and knowing if it is present within a mechanism will allow for greater control when attaching recognition systems to transducer surfaces. If the glycine containing peptides bind according to S_N2 kinetics, rates constants can be compared to see how much sterics impact the attachment reaction. The rate limiting step in this reaction is histidine substituting with the tethered NHS ester. Knowing this, changes in rate constant between histidine, his-gly and gly-his-gly will be attributed to the sterics around the nucleophilic histidine making the molecular orientation needed for substitution less likely. The rate comparisons will give a quantitative value to the effect of sterics on larger proteins that will help with protein recognition system selection in future biosensors. Additionally, with the structure of glycine being known, predictions can be made about how other amino acids attached to histidine could impact attachment. If this is the case, other histidine based peptides with more sterically hindered side chains can be tested to find where the cutoff point is that S_N1 attachment is invoked. Generally, more information about how quickly and efficiently larger histidine containing proteins being used as biosensor recognition systems will bind to surfaces through NHS/EDC tethering will be found.

Experimental Design

Overview

So far within the project, valid AgNP surfaces were found to conduct reactions on. Trials of histidine and his-gly were conducted using the NHS/EDC prepared AgNP surfaces and SERS. Observed rate constants were found for histidine and his-gly trials, but more trials must be conducted in order to produce statistically sound results. More trials involving different peptides are planned to be conducted in the future as well.

Synthesis of Nanoparticle Surfaces

The AgNP were synthesized and then filtered onto a membrane to create surfaces.[35] BNNS is made by sonicating boron nitride solution (0.2037 g BN, 100 mL E-Pure H_2O) overnight. The mixture was then centrifuged for 1 hour at 5000 rpm and 3℃. The clear part of the centrifuged solution was decanted off and used in synthesis. 5 mL of silver nitrate solution (0.0425 g $AgNO_3$, 25.0 mL E-Pure H_2O) were mixed with 5 mL of BNNS in solution in a 25 mL beaker.[30] 6 mL hydrazine monohydrate solution (4.86 µL hydrazine monohydrate, 50 mL E-Pure H_2O) was added to a buret.[30] Hydrazine monohydrate was used in efforts of keeping AgNP from becoming too large.[22] Stronger reducing agents act too quickly, which can create non-uniform AgNP surfaces upon filtration. For this reason, the hydrazine solution was slowly dripped into the stirring silver nitrate/BNNS mixture over the course of 30 minutes (Figure 5A). The resulting solution was filtered through a Millipore Stainless Steel Filter Holder onto 0.8 mm polycarbonate membrane filters in 5 mL parts (Figure 5B). 5 mL of E-Pure water was then passed through the filtration apparatus, then the membrane filters were removed. The AgNP surface on

the membrane filter should be uniformly dispersed and dark blue/grey in color when removed from the apparatus (Figure 5C).

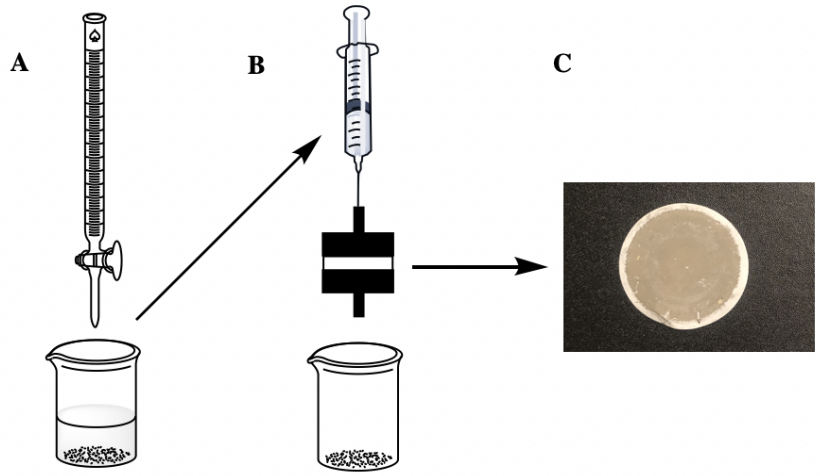


Figure 5: A shows the hydrazine solution being dripped into the stirring $AgNO_3$/BNNS solution below. The resulting solution is then passed through the filtration apparatus in **B**, with waste being collected below. **C** is an image of a final AgNP surface after being soaked in 4-MBA solution.

The surfaces were dried, then immediately soaked in a 1 mM 4-MBA (7.70 mg 4-MBA, 50 mL Ethanol) for 20 minutes. Surfaces can be dried and stored in the refrigerator after this step. The surfaces were then soaked in an equal part by volume (10 mL each) mixture of 0.001 M NHS (9.2 mg NHS, 20 mL E-Pure Water) and 0.01 M EDC (7.67 mg EDC, 20 mL E-Pure Water) solution for an additional 20 minutes. The NHS/EDC soak needs to be performed immediately before trials with histidine containing peptide reactions to prevent the NHS peak from degrading over time. It should be noted that these surfaces age, and should be remade every one to two weeks in order to maintain the highest Raman enhancement possible.

Trials with Peptides

All peptide solutions were made using a pH 7 sodium phosphate buffer solution (100 mL 0.1 M Na_2HPO_4, 63.1 mL 0.1 M HCl). 20 mM Stock Solution of histidine (0.1552 g histidine, 50 mL pH 7 phosphate buffer), and his-gly (0.040 g his-gly, 7.5 mL pH 7 phosphate buffer) were made. The 25 mM his-gly stock solution was refrigerated when not being used. The NHS/EDC solution soaked surfaces were placed under a running Sierra Snowy Instruments Desktop Raman Spectrometer at an integration time of 10.00 s. Initial NHS and 4-MBA peak heights were recorded. 1 mL of the peptide solution was deposited onto the surface using a plastic syringe and added to one location on the surface. Raman spectra was collected every 30 seconds for the first 5 minutes, 60 seconds from 5-20 min and 120 seconds from 20 min to finish. The overall setup of trials is shown in Figure 6. The reaction was left to run for 30-40 minutes, until NHS peak appeared to stop decreasing in size.

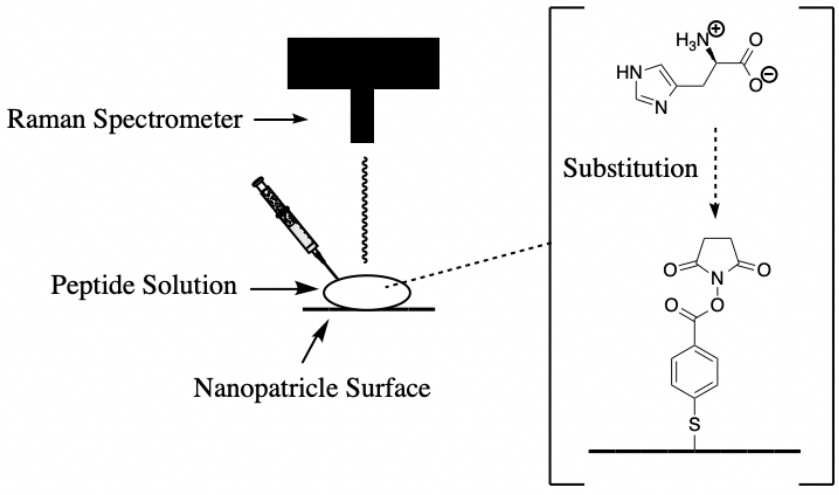


Figure 6: The histidine solution is administered to AgNP surfaces. The histidine molecules diffuse to the tethered biosensor where S_N2 reactions with the activated ester take place.

After a trial took place, the Raman data was processed in order to determine the rate constant. This was all completed using the computer software Kaleidagraph. As the reactions progressed, there was less NHS on the surface, which made the height of the NHS succinimide peak around 1770 cm^{-1} decrease.[12] Since the amount of the benzene group within the 4-MBA molecule on the surface remains unchanged, the peak around 1590 cm^{-1} remained constant. Tracking the peak height ratio of the NHS peak over the 4-MBA as the reaction progressed made sure that the potential fluctuating height within the Raman spectra was taken into account. Histidine and glycine do not have Raman peaks close to the NHS or 4-MBA peaks being observed, so even as the peptides bound to the surface, there should be no interference.[25,34] The ratio of the peaks was graphed vs time and fit to an exponential decay equation (Eq 3). This is where Y is the 1770/1590 peak ratio, e is Euler's number, k is the observed rate constant, t is time in seconds, and b is the "dark" signal not due to the NHS.

$$Y = Y_o e^{-kt} + b \quad \textbf{(3)}$$

The observed rate constants for each peptide were then graphed with respect to concentration. The graphs were fitted to see if they exhibit the integrated rate law for either a first (Eq 4A) or second order (Eq 4B) reaction.

$$k_{obs} = k \quad \textbf{(4A)}$$

$$k_{obs} = k\,[Peptide\ Concentration] \quad \textbf{(4B)}$$

The actual rate constant was used to make comparisons between reactions of different peptides. All trials of other histidine containing peptides will follow the same procedure.

A key component of the trials of histidine containing peptides is that peptide solutions are made to be at pH 7. There are multiple sites within the peptides that could engage in nucleophilic attack on the NHS ester but at pH 7, it will most likely be the imine nitrogen within the side chain of histidine. This is because histidine has three pKas; the carboxyl end has a pKa of 1.82, amino end 9.17, and the side chain 6.00.[26] It has been proven that reactions involving histidine, or peptides including glycine and histidine are effective nucleophiles within the 6.5-8 pH range.[36] Since the pH is above the pKa of the side chain and the carboxyl group of histidine, they will be deprotonated. The amino group of histidine will be protonated, and not able to nucleophilically attack. Even though deprotonated, the carboxyl is also predicted to not preferentially attack compared to the side chain of histidine. It is not as strong as a nucleophile as the deprotonated nitrogen. The carboxyl group has a polarizable delocalized negative charge at pH 7, that makes it less likely to be the competitive nucleophile. The nitrogens within the histidine side chain are also less electronegative than the oxygens in the carboxyl, which makes for a stronger nucleophile.[37]

As seen in Figure 2A, there are imine (C=N) and allylic (HN-C) nitrogens within the side chain of histidine. While both nitrogens have lone pairs that can participate in nucleophilic attack, the lone pair on imine is more likely to. The imidazole ring of histidine has a conjugated pi system between the various carbon and nitrogen atoms within it. The lone pair of the allylic nitrogen is in the p orbital, and tied up within the conjugated pi system. Conversely, the lone pair of the imine nitrogen is in the sp^2 orbital, and is orthogonal to the conjugated pi system. Since it is outside of the pi system of the imidazole ring, it is more likely to engage in nucleophilic of the NHS ester. The pH of the peptide solutions should be regularly checked with litmus paper before trials are conducted. Checking pH makes sure it is the imine nitrogen within the histidine side chain participating in nucleophilic attack of the adsorbed NHS ester.

Preliminary Results

Trials With Histidine

Trials involving concentrations of histidine (5-20 mM) were conducted using SERS to obtain information about the rate law and rate constant. Through the various trials of histidine, a steady decay of the NHS peak around 1770 cm^{-1} with respect to the constant 4-MBA phenyl ring peak around 1590 cm^{-1} was observed. Figure 7 shows the exponential decay fits of the peak ratio vs time as different concentrations of pH 7 histidine solution are introduced to the NHS ester prepared AgNP surfaces.

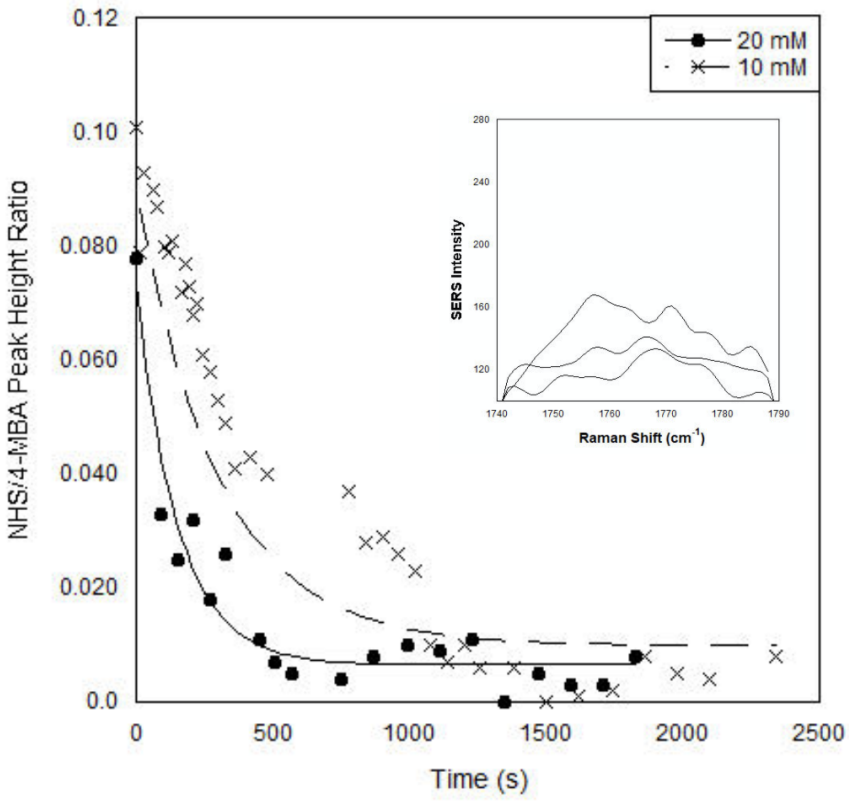


Figure 7: It is shown that there is a more rapid decay of the NHS peak at higher (20mM) concentrations compared to lower (10 mM). Shown within the inset is the real time degradation of the NHS peak around 1770 cm^{-1}.

The observed rate constants for all histidine trials were obtained through the exponential decay fit in Eq 3. The k_{obs} were averaged then graphed with respect to histidine concentrations to obtain actual rate constant. Figure 8 shows the linear regression for k_{obs} with respect to histidine concentration.

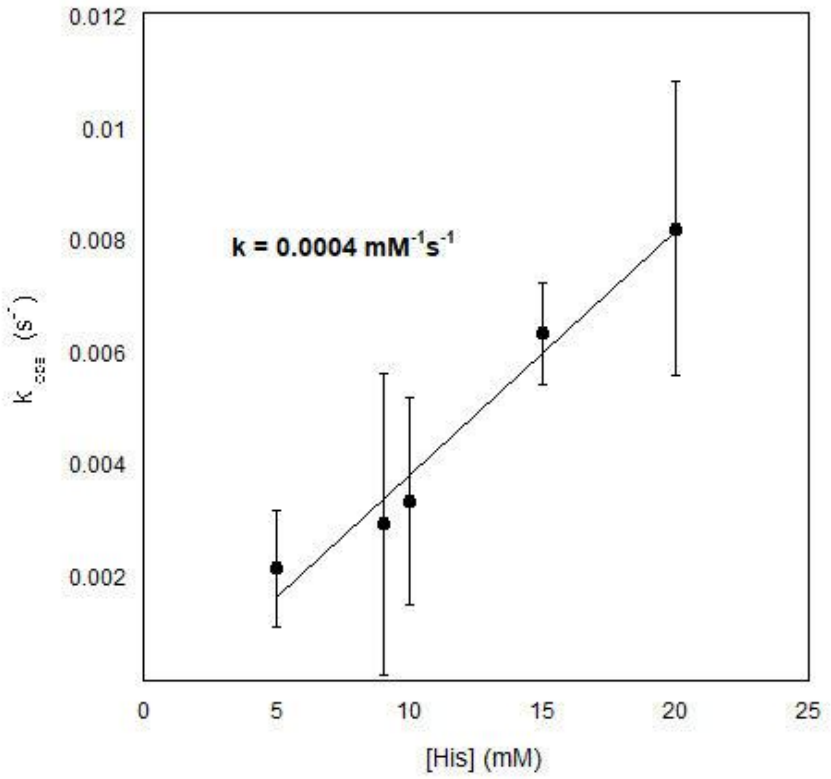


Figure 8: The graph of observed rate constant vs Histidine concentration is fitted to y = -0.00058 + 0.0004x R=0.985. The error bars represent standard deviation of 3-5 trials.

The linear regression supports that the attachment reaction is dependent upon histidine and NHS ester concentration. This provides evidence for a second order rate law, and the proposed S_N2 mechanistic pathway of peptide attachment. However, with the large error bars, more data is needed before the k = 0.0004 $mM^{-1}s^{-1}$ rate constant can be confirmed. All k_{obs} values put into averages were checked for significance using Grubbs' test for outliers. Specifically, k_{obs} for concentrations of 20 mM and 10 mM

deviated more than others. Averages must be made tighter and/or more outliers must be removed before a rate constant can be definitively proven. Regardless, the current linear trend for singular histidine trials, and the rough estimate of a rate constant shows that Specific Aims 1 and 2 are feasible.

Trials With Histidine-Glycine

Trials involving concentrations of histidine (5-25 mM) were conducted using SERS to obtain information about the rate law and constant. Similar fits that to the exponential Eq 3 were seen with his-gly and histidine. Figure 9 shows a difference in histidine peak rate of decay across two different concentrations of his-gly.

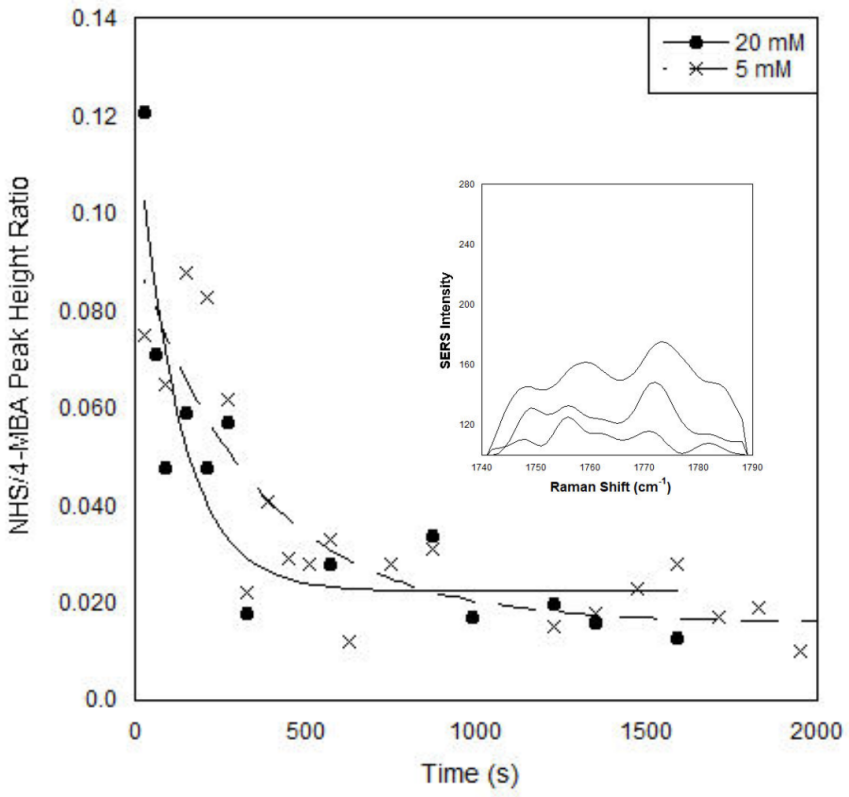


Figure 9: It is shown that there is a more rapid decay of the NHS peak at higher (20 mM) concentrations compared to lower (5 mM). Shown within the inset is the real time degradation of the NHS peak around 1770 cm^{-1}.

There was more noise in spectra, creating higher variance within trials of his-gly compared to histidine. The ranges of k_{obs} values were larger within one concentration. However on average, the k_{obs} values for his-gly were slightly lower compared to singular histidine attaching to the surfaces. Figure 10 shows the k_{obs} vs his-gly concentration data for all trials.

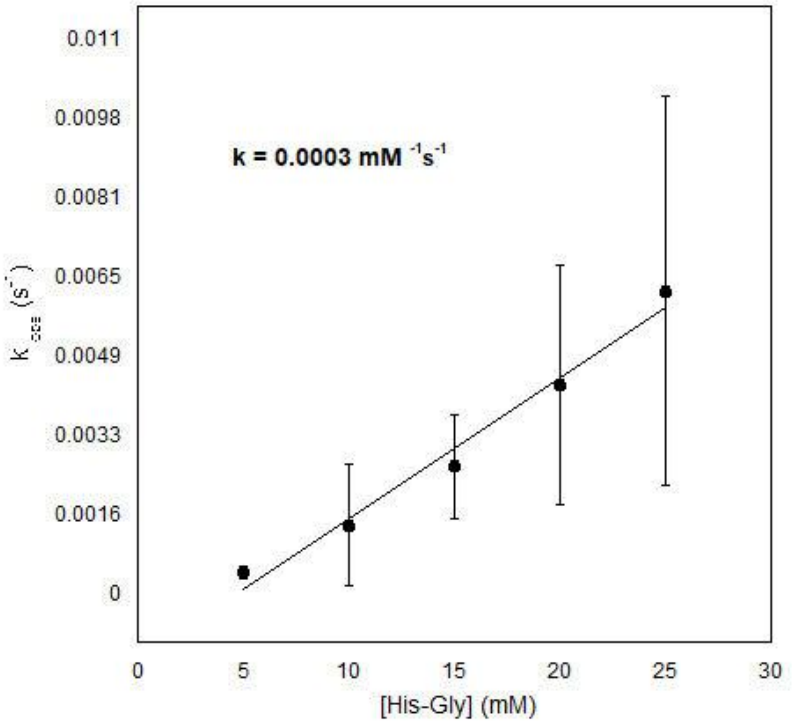


Figure 10: The graph of observed rate constant vs Histidine concentration is fitted to y = -0.0013 + 0.0003x R=0.99. The linear regression proves a second order rate law of Histidine-Glycine attachment.

Again, the close fit to a linear regression provides evidence that his-gly attachment is dependent upon both NHS ester and peptide concentration. However, even after Grubbs' test for outliers, the large error bars show high amounts of variance between trials of the same concentrations. It is difficult to conclude the rate constant of k = 0.0003 $mM^{-1}s^{-1}$ definitely, but it shows Specific Aim 3 is attainable.

Overall Conclusions

The first major takeaway from the study is that comparisons can be made between the histidine substitution with NHS tethered AgNP on surfaces, versus those existing in solution. It was found previously that histidine reacts with NHS esters on AgNP surfaces in solution according to S_N2 kinetics. The rate constant for this reaction was 0.076 $mM^{-1}s^{-1}$.[12] The current rate constant found for the same reaction on surfaces instead of solution was 0.0004 $mM^{-1}s^{-1}$. As stated previously, this rate constant for surface reactions cannot be definitely concluded due to high variance between trials. However, even if just an estimate, the current surface reaction rate constant was two orders of magnitude smaller than in solution. Even if variance is lessened by removal of outliers from more trials, it is unlikely that the difference in magnitude between surface and solution reactions would change. It shows that the reactions happen much slower on surfaces and begins to answer Specific Aim 2. As predicted, when the histidine and tethered NHS esters are able to freely move through solution, they are more likely to interact in a way that leads to reaction. When the NHS ester is immobilized, it significantly decreases the rate of reaction. Once rate constant is definitely proven, it will allow for predictions to be made about how much longer, and less efficient a reaction will be when one of the reagents are immobilized on a metal nanoparticle surface.

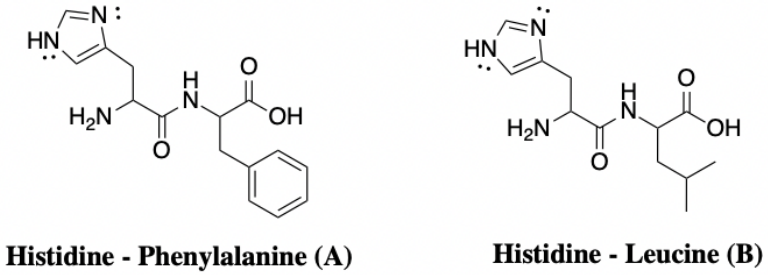
Another major takeaway is that so far, evidence points to histidine and his-gly binding to NHS tethered AgNP surfaces according to S_N2 kinetics. As stated previously, the linear regression for both shows evidence towards the reactions being dependent upon tethered NHS ester and peptide concentration. Histidine binding in a S_N2 mechanism is specifically important to prove because it will be what rate laws and constants of all other peptides tested are compared to. Additionally, since both histidine and his-gly both show evidence that they follow the same rate law supports that a single glycine residue is not enough of a steric inhibitor to invoke mechanistic change. While his-gly is objectively larger than singular histidine, it is nowhere close to the size of glucose oxidase that follows S_N1

attachment.[12] While his-gly (212.21 g/mol) is a mere dipeptide, glucose oxidase is a much larger protein consisting of 583 residues (160 kDa).[38-39] Due to how similar the histidine and his-gly data are, the gly-his-gly tripeptide (269.26 g/mol) will also probably not be enough to significantly produce a change in rate law or constant.[40] However, while it appears that the tested peptides follow a second order mechanism, this cannot be definitively proven until error bars showing standard deviation are reduced. The same thing is true for current rate constants. While data shows that histidine has a slightly higher rate constant compared to his-gly, there is too much variance within the current data to make that conclusion definitively.

Proposals For Future Research

Moving forward, there are a few recommendations for this study based on preliminary findings. Firstly, more trials of histidine and his-gly on surfaces must take place. While rate constants of 0.0004 $mM^{-1}s^{-1}$ and 0.0003 $mM^{-1}s^{-1}$ were obtained respectively, the error bars seen within the graphs were very large at some concentrations. Specifically 20 mM, 10 mM histidine trials and 25, 20 and 10 mM trials of his-gly should be revisited to reduce the size of the error bars. While both histidine and his-gly k_{obs} vs peptide concentration graphs fit a linear regression for a second order rate law, more trials will prove that the rate constants are significantly different. Not enough data has been collected currently to conclusively prove that histidine attaches at a faster rate compared to his-gly. If variance continues in future trials, peptide solutions could be made in a non-nucleophilic base solution or higher pH values. As the reaction progresses, histidine is deprotonated by H_2O in solution before it engages with the NHS ester. If it were in basic solution, the histidine would be more likely to be deprotonated initially, and not engage in acid/base reactions with solvent protons. This could make the reaction proceed more rapidly which could lead to less fluctuation in peaks seen specifically towards the end of trials.

An additional proposal for research is to attempt trials with other histidine based peptides that have larger side chains than glycine. It is recommended that other peptides be tested alongside or instead of gly-his-gly due to how similar data between histidine and his-gly appears. In Figure 11, some histidine based peptides are shown that can be explored for their reactions with tethered NHS esters on AgNP surfaces.



Histidine - Phenylalanine (A) **Histidine - Leucine (B)**

Figure 11: Molecular structures of histidine-phenylalanine (His-Phe) and histidine-leucine (His-Leu) are shown. The side chains of which will provide more competing steric bulk compared to that of glycine.

The phenyl substituent on his-phe and the isopropyl like group on his-leu would be introducing more sterics compared to the hydrogen side chain of glycine. These have the potential to impact the rate constant more significantly so quantitative comparisons can be made to single histidine. Since they are small dipeptides, they will more than likely still bind to the surfaces according to S_N2 kinetics based on the his-gly data, just at a slower rate. While other dipeptides could also introduce more sterrics than glycine, like histidine-tryptophan or histidine-tyrosine, they would introduce new nucleophiles that could compete with histidine attachment. If glycine is desired to be the amino acid that contributes to sterrics, a potential five member (Gly-Gly-His-Gly-Gly) or 7 member (Gly-Gly-Gly-His-Gly-Gly-Gly) glycine substituted histidine centered peptide could be used. These have the ability to hinder the nucleophilic histidine attaching more significantly than his-gly. There also is more of a chance for these 5 and 7 member peptides to act as a larger protein that attaches via S_N1 as more peptides are present to hinder histidine in the attachment reaction. Overall, the preliminary data shows conclusive evidence that there is

more to be found from the study of how sterics impact the mechanism of histidine peptide attachment to NHS ester prepared AgNP surfaces. The research so far has the ability to positively impact the field of biosensing technology and there is strong hope by the author for it to be continued.

Acknowledgements

I would like to firstly acknowledge Dr. Alice Deckert for all of the help that she has given me with this project and teaching me the material needed to complete it. It has not been an easy journey, but through countless meetings full of very helpful advice, I am very happy and proud of this work that we have accomplished together on this project. Thank you very much for being such a great mentor from Chem 120, all the way to my senior project. I would also like to recognize Dr. Betush for the assistance with this project and overall advice through my time at Allegheny. Additionally, I would like to thank Dr. Murphree for teaching me information needed to complete this project as well. Organic 1 and 2 was a pivotal time in my academic career, and it showed me the amount of dedication needed if I sought to be successful in the field. I would also like to acknowledge all those who have worked on similar projects before me in the Deckert Lab group, like Lizzie and Zoe. They helped show me the ways of the lab when I was just a sophomore entering the field of undergraduate research. An additional acknowledgement goes to my family at home. A huge thank you to my father, mother, sister, grandparents, aunts, uncles, and cousins have been so supportive of all of my academic endeavors. I could not be thankful enough for the opportunities they have given me. My grandfather, Charles Blackburn, an Allegheny alumni was also a strong influence in my undergraduate selection. I am grateful that he showed me how wonderful of an institution this school is. Lastly, I would like to thank all of my friends I have made through the years at school. This goes to members of the swim team like Mcclaren, Miranda, Justin, Daniel, Emily, Anna, Aimee, Ariana, Willa and Chelsea who have been there for me in and out of the water. Stay bad! This also goes for my fellow fraternity brothers like Jake, John, Matt and David that have been there for me during times of crisis and celebration. You all have been the highlight of my college experience, and I would have not made it through all of the academic hardships without the great times we have shared together. Also my dog Deliliah, you are my guiding light.

References

1. In *Bioprocess technology* (1991), vol. 15, pp. 1–344. Blum Loïc J. & Coulet, P. R. in *Biosensor principles and applications* 1–6 (M. Dekker, 1991).

2. K. E. Shafer-Peltier, C. L. Haynes, M. R. Glucksberg, R. P. Van Duyne, Toward a glucose biosensor based on surface-enhanced Raman scattering. *Journal of the American Chemical Society*. **125**, 588–593 (2003).

3. Wei, Q., Lin, J., Liu, F., Wen, C., Li, N., Huang, G., & Luo, Z. (2019). Synthesis of MBA-encoded silver/silica core-shell nanoparticles as novel SERS tags for biosensing gibberellin A3 based on AuFe3O4 as substrate. *Sensors (Switzerland)*, *19*(23).

4. A. M. Hada *et al.*, Fabrication of gold-silver core-shell nanoparticles for performing as ultrabright SERS-nanotags inside human ovarian cancer cells. *Nanotechnology*. **30** (2019), doi:10.1088/1361-6528/ab1857.

5. B. Pejcic, R. D. Marco, G. Parkinson, The role of biosensors in the detection of emerging infectious diseases. *Analyst*. **131** (2006), pp. 1079–1090.

6. A. J. Kimple, R. E. Muller, D. P. Siderovski, F. S. Willard, A capture coupling method for the covalent immobilization of hexahistidine tagged proteins for surface plasmon resonance. *Methods in molecular biology (Clifton, N.J.)*. **627**, 91–100 (2010).

7. Y. Zheng, Y. Lin, Y. Zou, Y. Yang, C. Wang, Peptide-/protein-mediated nano-bio interface and its applications. *Kexue Tongbao/Chinese Science Bulletin*. **63**, 3783–3798 (2018).

8. M. K. Sharma *et al.*, A novel piezoelectric immunosensor for the detection of malarial Plasmodium falciparum histidine rich protein-2 antigen. *Talanta*. **85**, 1812–1817 (2011).

9. M. Li *et al.*, Site-Specific and Covalent Immobilization of His-Tagged Proteins via Surface Vinyl Sulfone-Imidazole Coupling. *Langmuir*. **35**, 16466–16475 (2019)

10. C. Ley, D. Holtmann, K. M. Mangold, J. Schrader, Immobilization of histidine-tagged proteins on electrodes. *Colloids and Surfaces B: Biointerfaces*. 88 (2011), pp. 539–551.
11. GE Healthcare Life Sciences, Approaches for capture of histidine tagged proteins in Biacore™ systems. *Amershambiosciences.Biz*, 6 (2011).

12. A. A. Deckert, K. A. Anderson, K. M. Mullaugh, C. Delaney, Comprehensive study of the formation and reaction of a tethered N-hydroxysulfosuccinimidyl ester used to covalently tether proteins to surfaces. *Journal of Physical Chemistry B*. 108, 15808–15814 (2004).

13. J. K. Lim, Y. Kim, S. Y. Lee, S. W. Joo, Spectroscopic analysis of l-histidine adsorbed on gold and silver nanoparticle surfaces investigated by surface-enhanced Raman scattering. *Spectrochimica Acta - Part A: Molecular and Biomolecular Spectroscopy*. 69, 286–289 (2008).

14. C. Gellini, G. Sabatino, A. M. Papini, M. Muniz-Miranda, SERS study of a tetrapeptide based on histidine and glycine residues, adsorbed on copper/silver colloidal nanoparticles. *Journal of Raman Spectroscopy*. 45, 418–423 (2014).

15. H. Ma *et al.*, Surface-enhanced Raman scattering for direct protein function investigation: Controlled immobilization and orientation. *Analytical Chemistry*. **91**, 8767–8771 (2021)

16. A. Arafat, M. A. Daous, A short route of covalent biofunctionaliztion of silicon surfaces. *Sensors and Actuators, B: Chemical*. 152, 226–234 (2011).

17. V. Martinez-Luaces, in *Chemical Kinetics* (InTech, 2012).

18. Elementary Reactions https://chem.libretexts.org/@go/page/1410 (accessed Apr 20, 2021).

19. Pseudo-1st-order reactions https://chem.libretexts.org/@go/page/1441 (accessed Mar 26, 2021).

20. 1. O. A. El Seoud, W. J. Baader, E. L. Bastos, in *Encyclopedia of Physical Organic Chemistry, 5 Volume Set* (John Wiley & Sons, Inc., 2016), pp. 1–68.

21. X. F. Zhang, Z. G. Liu, W. Shen, S. Gurunathan, Silver nanoparticles: Synthesis, characterization, properties, applications, and therapeutic approaches. *International Journal of Molecular Sciences*. **17** (2016), , doi:10.3390/ijms17091534

22. U. Nickel, A. Z. Castell, K. Pöppl, S. Schneider, Silver colloid produced by reduction with hydrazine as support for highly sensitive surface-enhanced Raman spectroscopy. *Langmuir*. **16**, 9087–9091 (2000).

23. S. Campisi, M. Schiavoni, C. E. Chan-Thaw, A. Villa, Untangling the role of the capping agent in nanocatalysis: Recent advances and perspectives. *Catalysts*. **6** (2016), , doi:10.3390/catal6120185.

24. Hard and Soft Acid and Base Theory https://chem.libretexts.org/@go/page/192314 (accessed Apr 22, 2021).

25. J. G. Smith, P. K. Jain, The ligand shell as an energy barrier in surface reactions on transition metal nanoparticles. *Journal of the American Chemical Society*. **138**, 6765–6773 (2016).

26. A. L. Hansen, L. E. Kay, Measurement of histidine pKa values and tautomer populations in invisible protein states. *Proceedings of the National Academy of Sciences of the United States of America*. **111** (2014), doi:10.1073/pnas.1400577111.

27. Cooksy, A. (2014) Raman Spectroscopy, in *Physical chemistry: Quantum chemistry and molecular interactions*, pp 292–296. Pearson Boston, MA.

28. Applications of Raman Spectroscopy https://chem.libretexts.org/@go/page/74390 (accessed Apr 18, 2021).

29. H. Yockell-Lelièvre, F. Lussier, J. F. Masson, Influence of the Particle Shape and Density of Self-Assembled Gold Nanoparticle Sensors on LSPR and SERS. *Journal of Physical Chemistry C*. **119**, 28577–28585 (2015).

30. Y. Lin, C. E. Bunker, K. A. S. Fernando, J. W. Connell, Aqueously dispersed silver nanoparticle-decorated boron nitride nanosheets for reusable, thermal oxidation-resistant surface enhanced Raman spectroscopy (SERS) devices. *ACS Applied Materials and Interfaces*. **4**, 1110–1117 (2012).

31. Homola, J. Present and future of surface plasmon resonance biosensors. *Anal Bioanal Chem* 377, 528–539 (2003).

32. Surface Structures- fcc Metals https://chem.libretexts.org/@go/page/25356 (accessed Apr 22, 2021).

33. C. Tan, Z. Zhang, Y. Qu, L. He, Ag2O/TiO2 Nanocomposite Heterostructure as a Dual Functional Semiconducting Substrate for SERS/SEIRAS Application. *Langmuir*. **33**, 5345–5352 (2017)

34. J. S. Suh, M. Moskovits, Surface-Enhanced Raman Spectroscopy of Amino Acids and Nucleotide Bases Adsorbed on Silver. *Journal of the American Chemical Society*. 108, 4711–4718 (1986).

35. I. H. Kim *et al.*, Tuning the interparticle distances in self-assembled gold nanoparticle films with their plasmonic responses. *Chemical Physics Letters*. **715**, 91–99 (2019).

36. L. F. Wong, J. C. Cooper, D. W. Margerum, Kinetics of Copper(II)-Glycylglycyl-L-histidine Reactions. Acid Decomposition and Proton-Assisted Nucleophilic Displacement by Triethylenetetramine. *Journal of the American Chemical Society*. **98**, 7268–7274 (1976).

37. Klein, D. R. (2021) Nucleophilic Strength and Solvent Effects in S_N2 Reactions, in *Organic chemistry*, pp 285–287. WileyHoboken, NJ.

38. Sigma Aldrich. (2020) Gly-his. Product *Information.*

39. Sigma Aldrich. (2020) Glucose Oxidase. *Product Information*.

40. Sigma Aldrich. (2020) Gly-His-Gly. *Product Information*.